THE OCCURRENCE OF PALYGORSKITE IN THE YUCATÁN PENINSULA: ETHNO-HISTORIC AND ARCHAEOLOGICAL CONTEXTS*

M. SÁNCHEZ DEL RÍO

European Synchrotron Radiation Facility, BP 220 F-38043 Grenoble Cedex, France

M. SUÁREZ

Departamento de Geología, Universidad de Salamanca, E-37008 Salamanca, Spain

and E. GARCÍA-ROMERO

Departamento de Cristalografía y Mineralogía, Universidad Complutense de Madrid, E-28040 Madrid, Spain

Palygorskite is a rare clay mineral used by the ancient Mayas for fabricating the Maya blue pigment and for other purposes. It seems to have been obtained from a restricted area in the Yucatán peninsula where important archaeological sites are found. Geological samples from different localities in this area show a high content in palygorskite, indicating that this clay is widespread in Yucatán. Combining structural, morphological, compositional and geochemical methods, we analysed the common characteristics of Yucatecan palygorskites, and compared them with palygorskites from other origins around the world. These results can be used for defining a fingerprint of Yucatecan palygorskite to be used in provenance studies of archaeological artefacts, in particular the Maya blue pigment.

KEYWORDS: PALYGORSKITE, YUCATÁN, MAYA CULTURE, MAYA BLUE

INTRODUCTION

The Yucatán peninsula is mainly formed by marine carbonated sediments. A Tertiary calcareous sequence crops out in a large part of Yucatán without significant deformation and appears as a calcareous plateau slightly inclined to the north-west. This is the direction in which the Cenozoic units (Tertiary mainly) showed a gradual retreat of the sea towards the present line of the coast (Morán-Zenteno 1994). This is a karstic zone that does not have water at the surface (rivers or lakes) and the underground water is accessible at sinkholes produced by the falling of the surface rock. These important formations are locally called *cenotes* (from the Mayan *dzonot*, a well venerated by the ancients because it contained water that never saw the light).

This tropical peninsula was densely populated in the past. Archaeological findings have demonstrated that the ancient Maya created complex trade networks (Sabloff and Rathje 1975), systems of water storage and distribution (Scarborough and Gallopin 1994) and a sustainable system of agriculture. Many important Maya archaeological sites can be found in this area, in particular those corresponding to the Puuc (from the Mayan for 'hills') characterized by an architectural ornament at vault level, dating from the Late Classic Period (AD 800–1000).

Palygorskite is known since ancient times in Mesoamerica, in particular in the Mayan Lowlands. There are several fundamental facts that indicate that this material and its properties were very well known by the Maya and that it was linked to sociocultural aspects of the Maya culture. The first fact is that palygorskite (locally known as *sacalum*) is still known amongst the indigenous communities of the Yucatán peninsula (Yucatán and Campeche states) and is used for several applications, including ritual ceremonies (fabrication of candles used on the Day of the Dead), domestic and art craft ceramic production (pottery fabrication in the area of Ticul), and medical treatments. Its use as a curative agent (Bohor 1975) was both external for pain relief in cases of mumps and abdominal pain, and as a drug for dysentery diseases and also for pregnant women (Folan 1969). It is remarkable that palygorskite and other clays are also used in modern pharmacology as an anti-diarrhoeic (Viseras and López-Galindo 1999), as the Maya did more than 1000 years ago. These traditions, which survived for a number of centuries, also suggest that palygorskite was more intensively used in the past.

The most important use of palygorskite is as the main ingredient in the Maya blue pigment. It is made by embedding an organic colorant (indigo, obtained from the *Indigofera suffruticosa* plant, locally known as *añil* or *xiuquilitl*) in the clay matrix of palygorskite. The resulting compound has an extraordinary resistance to chemicals and environmental aggression. The Maya blue was invented by the Maya in the period from the sixth to the eighth century. It has been found in archaeological artefacts all over Mesoamerica, from the Gulf to the Pacific coasts, suggesting that the Maya exported the Maya blue to most Mesoamerican cultures, such as Olmec-Xicalanca, Totonac, Huastec and Aztec. It was also used in Colonial times for the decoration of convents and churches (Reyes-Valerio 1993), at least until the end of the 16th century. Even later, it was employed for decoration of civil buildings in Colonial Cuba (Tagle *et al.* 1990).

In this work, we study palygorskite samples collected in several locations in the Yucatán peninsula and compare them to other palygorskites from other sources in the world. The Yucatecan samples were not only obtained from sources well described in the literature, but also from new ones. The analysis of these samples aims to answer the following two questions: (i) Did the Maya mine palygorskite from one or a few well-located sources or, on the contrary, is palygorskite very frequent in Yucatán and could it have been obtained from many places? (ii) Does the Yucatecan palygorskite present mineralogical characteristics different from other origins that could be recognized in archaeological Maya blue?

MATERIALS

Prior to the retrieval of palygorskite samples, an exhaustive bibliographical search identified the possible historical sources. Many of these sources were studied in an ethno-historic context (Folan 1969; Arnold and Bohor 1975; Bohor 1975; Arnold 2005; Arnold *et al.* 2007). Using these data, we defined a searching area consisting of a circle of about 40 km radius, centred on the archaeological site of Uxmal (see Fig. 1). Most of the sites referred to in the literature lie inside this area.

The three most important sites are as follows:

- The *cenote* in a village called Sacalum. This is probably the best documented source (Arnold and Bohor 1975; Bohor 1975) because there is archaeological evidence of its use as a palygorskite mine in ancient times. In our visit to the *cenote*, we collected a sample (labelled Y19) from the debris of extraction work lying on the *cenote*'s floor, close to the entrance stair. Inside the *cenote*, there is a small entrance to a contiguous chamber of ~300 m^2, the mine, accessible via

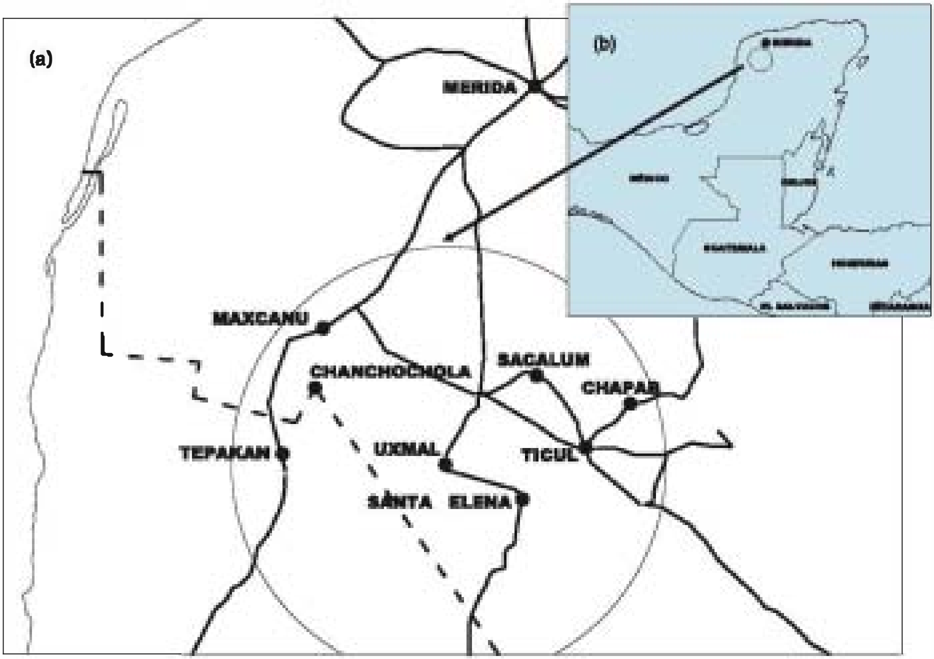

Figure 1 *(a) Detail of the region of interest (40 km around the Uxmal site), with indications of some localities. (b) A map of the Gulf of Mexico Gulf: the region of interest is encircled.*

a tunnel excavated in the palygorskite deposit (Bohor 1975). There is direct evidence that a high amount of palygorskite was extracted in the past. Local inhabitants informed us that although the mine is not exploited at present, some people occasionally enter to extract palygorskite for fabricating cosmetics. The sample Y8 was obtained from inside the mine.

- The Ticul–Chapab road. There are many sources of palygorskite along this road. They are well known by the potters of Ticul, who use palygorskite as temper for improving the characteristics (resistance to fracture) of their pastes (Arnold 1998). One site was studied in a geological context, sampling from existing prospection wells (Bohor 1975). We were not able to identify these wells. Another site is related to an ancient mine (Arnold 2005). Palygorskite from this zone, obtained from the Ticul potters, was used in recent works (Chiari *et al.* 2003; Giustetto *et al.* 2005; Sánchez del Río *et al.* 2006a). Three places were sampled. The first one, about 3–4 km from Ticul, on the right-hand side when looking in the direction of Chapab, could correspond to the old mine. It is located at coordinates N20°25.337′ W89°30.407′. We observed several cave-like holes in the floor, with direct evidence of extraction work in the past. A sample was taken (Y5) from the debris found on the floor. Another sample (Y6) comes from a second place, which is about 2 km further along the road, at N20°26.493′ W89°28.748′. A third place, about 7 km from Ticul, is much larger than all the others visited and has clear evidence of massive extraction of *sacalum*. It is at N20°26.567′ W89°28.643′. A sample (Y7) was collected from the tons of debris in this site. For the sake of completeness, we also included in the study another sample (Y0) from this zone, used in previous works (Sánchez del Río *et al.* 2005, 2006a,b; Suárez *et al.* 2007).

- Maxcanú. This site, a terrain cut on the railroad, is described by (Bohor 1975). We unambiguously identified it thanks to the pictures in Bohor (1975) and with the help of local people. The site is at N20°34.545′ W89°54.491′. It presents different rocky, powdered and sedimentary materials. We sampled different points: the sample Y1a comes from a sedimentary layer of approximately 2–4 cm. The sample Y1b is from a second point from the same layer. The samples Y1c and Y1d come from the contiguous bottom and top layers, respectively. The sample Y1e comes from another point close to the sedimentary layer. It looks to be the dominant material in the deposit, marked as ‘clay’ in figure 4 of Bohor (1975). Another layer was found with a very different colour (grey) and consistency (Y1f). Sample Y1g was taken from the other side of the railway.

Two new sites were sampled:

- A *sascabera* (N20°31.510′ W90°03.015′) close to Chanchocholá. This place is used at present for extracting *sascab*, calcareous material with good compaction characteristics, used for making roads. Two samples were taken, one from the predominant material (Y2a) and a second one (Y2b) looking very much like the samples Y1a and Y1b from Maxcanú.
- Sample Y3 was collected in a recent road cut along the new Uxmal–Mérida road (N20°23.336′ W89°46.172′).

A deposit in the Uxmal–Santa Elena road was cited in Arnold *et al.* (2007). We could not identify this exact place. Several road cuts exist and we sampled one (Y4) at N20°20.826′ W89°42.915′. This work also mentions two other sites: a *cenote* in Maní, also visited, but where we could not identify palygorskitic clays, and Mama, a village where we were also unsuccessful in finding the palygorskite source.

We also obtained materials from a pottery shop in Ticul: a sample of *sacalum* (Y9) and one of *sascab* (Y10), materials used systematically as temper for pottery. Another sample from Tepakan, Campeche (Y13) was also analysed.

In addition to the Yucatecan samples, for our mineralogical and chemical analyses we used other palygorskites from other origins: Bercimuel (BERC), Esquivias (E11), Torrejón el Rubio (TOR), Los Trancos (TRA) and Níjar (SNE) from Spain; Attapulgus (ATT) from Georgia (USA); and Lisbon (LISL) from Portugal. Most of these have been studied from other points of view (García Romero *et al.* 2006; Suárez and García Romero 2006).

ANALYTICAL METHODS

Mineralogical characterization was performed by X-ray diffraction (XRD), using a Siemens D 500 XRD diffractometer with Cu K_α radiation and a graphite monochromator. The samples used were random-powder specimens. They were powdered, but used ‘as found’, without any chemical treatment or washing. Powders were scanned in 2θ from 2° to 65° with a step of 0.02° and 3 s integration time.

Particle morphology and textural relationships were established by scanning electron microscopy (SEM) and transmission electron microscopy (TEM). SEM observations were performed using a JEOL JSM 6400 microscope, operating at 20 kV and equipped with a Link System energy-dispersive X-ray micro-analyser (EDX). Prior to SEM examination, freshly fractured surfaces of representative samples were air-dried and coated with Au under vacuum. TEM observations were performed by depositing a drop of diluted suspension on a grid of Ni with collodion.

The chemical composition was obtained by analytical electron microscopy (AEM) with TEM, in samples of great purity, using a JEOL 2000 FX microscope equipped with a double-tilt sample holder (up to a maximum of ±45°) at an acceleration voltage of 200 kV, with 0.5 mm zeta-axis displacement and 0.31 nm point-to-point resolution. The microscope incorporates an Oxford ISIS energy-dispersive X-ray spectrometer (136 eV resolution at 5.39 keV). Structural formulae for palygorskites have been calculated from the ideal structure, normalized to 42 negative charges. Oxygen was not measured quantitatively. All the Fe present in the samples was considered to be Fe^{3+}, thus neglecting the possible existence of Fe^{2+}, the content of which is usually very low.

The geochemical analyses were performed at the Activation Laboratory in Ontario (Canada). Major elements were obtained by Fusion-Inductively-Coupled Plasma (FUS–ICP) and trace elements were analysed using FUS–MS.

RESULTS AND DISCUSSION

The discussion here follows the different techniques used for obtaining complementary information on the Yucatecan palygorskite. The mineralogical characterization is discussed on the basis of the X-ray diffraction data. Morphological aspects, related to the fibrous structure, are unveiled by scanning electron microscopy (SEM). Electron microscopy was also used, this time in transmission mode (TEM), to obtain quantitative information about the chemical formula of the palygorskites (crystallochemistry). Last, the geochemistry analysis allows us to 'fingerprint' the Yucatecan palygorskites in a wider geological context, using both major and trace element concentrations. When studying archaeological Maya blue pigments, these results can be of great help for rejecting or accepting the hypothesis of Yucatecan provenance of the palygorskite.

Mineralogical characterization and phase purity (X-ray diffraction)

XRD diffractograms were recorded for all samples, and a semi-quantitative mineral analysis was performed. Table 1 shows the results of the mineral analysis. All samples present a very homogeneous composition, mainly palygorskite and carbonates (calcite and dolomite). Only two samples (Y1d and Y1f) from Maxcanú contain dioctahedric smectites and a third one (Y1g) contains small impurities of quartz. The two *sascab* samples can be described as palygorskitic marls, the sample from Chanchocholá is dolomitic, and the one from Ticul contain both calcite and dolomite. The high purity of palygorskite in most samples is remarkable.

The materials of the Maxcanú deposit are limestones and marls in which there are clay levels in thin layers (2–4 cm), very rich in palygorskite (Y1a and Y1b) or in dioctahedral smectite (Y1f). Calcite appears associated both with palygorskite and with smectite. Dolomite has not been identified in this zone.

None of the samples studied present palygorskite in combination with other clays (smectites, sepiolite etc.). The possible occurrence of sepiolite in Yucatán is an interesting matter, because sepiolite has been found in archaeological Maya blue pigments (Gettens 1962; Shepard 1962; Shepard and Gottlieb 1962). However, the presence of sepiolite is always related to blue pigments from the Valley of Mexico and it has never been found, to our knowledge, in Maya blue from the Maya region, an idea advanced by Shepard and Gottlieb (1962): 'It is noteworthy that sepiolite has not yet been found in any Yucatecan or Mayan sample.' The absence of sepiolite in Yucatán implies that the blue pigment containing sepiolite found in some archaeological artefacts does not incorporate Yucatecan palygorskite. We did not find sepiolite in our samples, in agreement with other studies on Yucatecan palygorskite (de Pablo-Galán 1996; Chiari *et al.* 2003). However, in the literature, the presence of sepiolite has occasionally been

Table 1 *The location of the samples and their mineralogical composition (Q, quartz; C, calcite; D, dolomite; S, smectite; P, palygorskite)*

Zone	*Location*	*Sample*	*Q*	*C*	*D*	*S*	*P*
West	Maxcanú	Y1a	–	–	–	–	100
		Y1b	–	–			100
		Y1c	–	100	–	–	–
		Y1d	–	50	–	50	–
		Y1e	–	100	–	–	–
		Y1f	–	–	–	100	–
		Y1g	<5	50	–	–	46
	Chanchocholá	Y2a	–	–	66	–	34
		Y2b	–	–	–	–	100
	Tepakan	Y13	–	–	–	–	100
Uxmal	Mérida–Uxmal road	Y3	–	8		–	92
	Uxmal – Santa Elena road	Y4	–	87	13	–	–
Ticul	Ticul–Chapab road	Y5	–	–	–	–	100
		Y6	–	–	–	–	100
		Y7	–	–	–	–	100
	Sacalum	Y8	–	–	–	–	100
		Y19	–	–	100	–	–
		Y0	–	–	–	–	100
	Pottery shop in Ticul	Y9	–	–	–	–	100
		Y10	–	34	20	–	46

reported in Yucatán, but not in surface outcrops. For instance, traces of sepiolite were found in the Chicxulub crater in Yucatán (Wolfgang *et al.* 2004), resulting from the impact of a meteorite that has been proposed as a cause of the extinction of the dinosaurs, about 60 million years ago. Isphording and Wilson (1974) found that sepiolite is frequently present in Yucatán, usually in small quantities, but it was the dominant material in some of the samples that they examined, such as one from Edzná (Campeche), a site located south of the region explored in this work.

Figure 2 shows the diffractograms of the samples with a high content or a full content of palygorskite. The similarities between all of them are remarkable. Although this observation may appear naive at first sight because the diffractogram is used to identify the mineral, it should be noted that clay minerals are characterized by a high compositional variability that is often related to structural variability and that, in turn, is demonstrated in the X-ray diffractogram. In particular, it was noted that although the diffractograms of different palygorskites are similar, their intensities and the total number of peaks are never the same (Chisholm 1990). Recently, Suárez *et al.* (2007) reported an empirical law that relates the chemical composition of the octahedral sheet of palygorskite with the cell dimensions: the greater the Mg concentration, the larger is the *a* parameter. Therefore, differences in composition imply a change in the *a* parameter, which in turn affects the position of some peaks in the diffractogram. These compositional differences affect mostly the two first peaks, corresponding to the 110 ($2\theta \approx 8°$) and 200 ($2\theta \approx 14°$) reflections.

The fact that two different palygorskites present different relative intensities could be related to a different proportion of the two crystallographic phases present in most palygorskites:

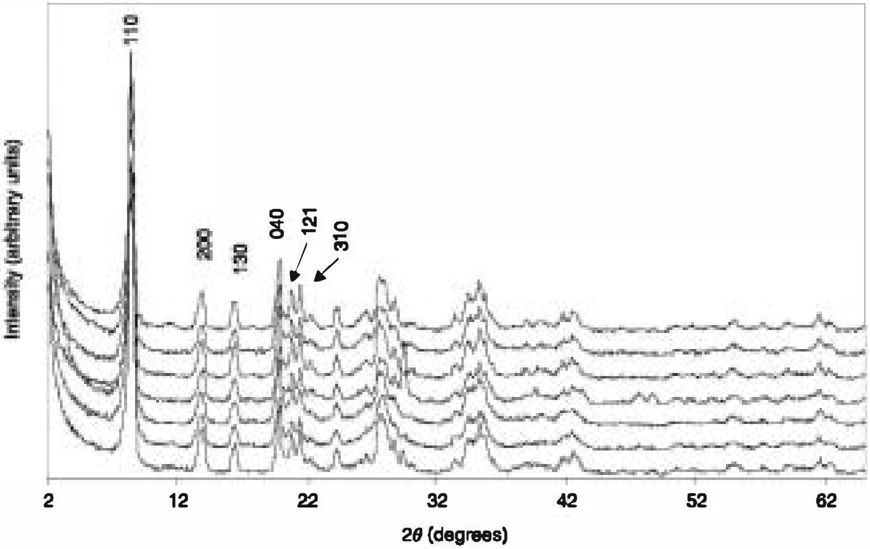

Figure 2 *X-ray diffractograms of the palygorskites with higher purity: from bottom to top, Y1a, Y2b, Y3, Y5, Y6, Y7 and Y8.*

monoclinic and orthorhombic (Chirst *et al.* 1969; Chisholm 1992; Chiari *et al.* 2003). This is particularly evident in the diffractogram region corresponding to peaks 130 ($2\theta \approx 16°$) and 040, 121 and 310 (in the region $2\theta = 19–22°$). As all of our samples present similar intensities, their ratio of the two crystallographic phases is very similar, with a slightly higher concentration of the monoclinic phase—we obtained 55–65% monoclinic from Rietveld refinement, depending on the fitting conditions, in agreement with Chiari *et al.* (2003) and Giustetto and Chiari (2004).

From the similarity of the diffractograms amongst the Yucatecan palygorskites, we deduce similar composition, as well as a similar presence of crystallographic phases. These two facts constitute well-defined characteristics of the Yucatecan palygorskites. To confirm the validity of this hypothesis, we calculated peak positions for the 110 and 200 reflections and the relative intensities of the 110, 200, 130, 040, 121 and 310 reflections for the Yucatecan palygorskites and the other reference palygorskites. The scatterplot matrix (Fig. 3) always shows the Yucatecan samples grouped, forming clusters that are distinguished from the others. This confirms the great homogeneity of the Yucatecan palygorskite group with respect to the other palygorskites, both from the compositional and the structural points of view.

The morphology and texture of palygorskite (scanning electron microscopy)

Microtextural images by SEM show that the samples studied look similar and present the characteristic fibrous morphology of palygorskite (Fig. 4). One can appreciate the high purity of the samples. The fibres of palygorskite are joined forming small bundles of 1–5 μm in length. These small bundles are arranged in parallel planes, with the *c*-axis (along the fibre axis) randomly oriented. The clay is formed by planar aggregates of bundles (Fig. 4 (b)) showing the characteristic texture of the sedimentary palygorskite. From this point of view, the Yucatán

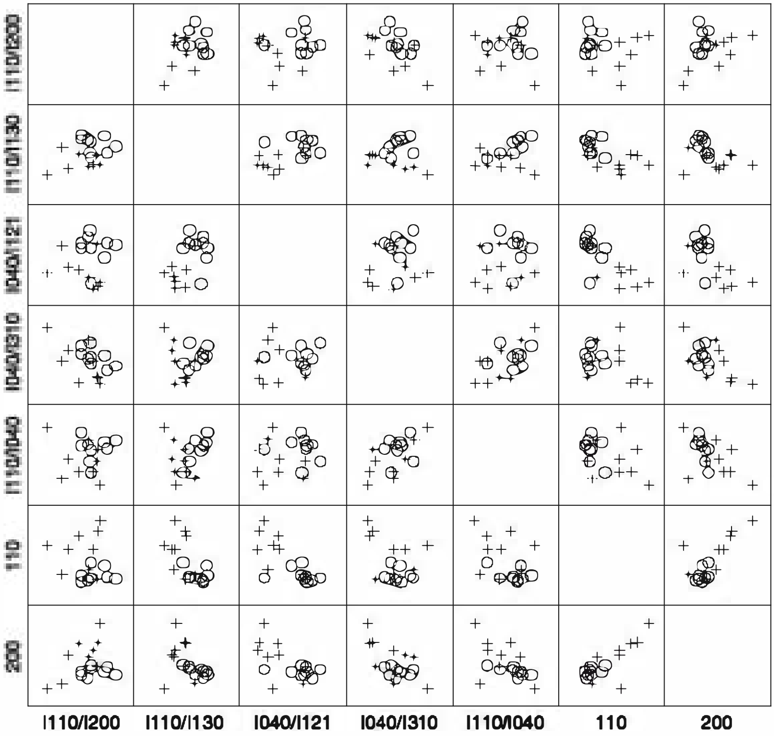

Figure 3 *A scatterplot matrix, which could be considered as the graphical equivalent of the correlation matrix, with the projections of the d-spacing of 110 and 200 reflections, which are affected by the composition, as discussed in the text, and the intensities I110, I200, I130, I040 and I121, which could be related to the different ratio of the orthorhombic and monoclinic phases in palygorskite. Each cell is a single plot, where the Yucatecan samples are marked with open circles (●) and palygorskites from other locations are marked with plus signs (+). Note that the Yucatecan palygorskites (●) group together in most cells.*

palygorskite is similar to the other sedimentary palygorskites used as references (such as Bercimuel, Torrejón or Esquivias).

Although a geological study of the deposit is beyond the scope of this work, the texture of the palygorskites of the Ticul area suggests a depositional formation process from solution. Moreover, the high purity of the palygorskite samples, the absence of quartz and smectites, and the spatial relation of the fibre planes to carbonate levels would also support this origin by direct precipitation from solution. Therefore, there is no sign of any transformation processes in the samples studied here (Y7, Y8 and Y13), even though other authors (Bohor 1975; Isphording 1984; de Pablo-Galán 1996) have proposed that some Yucatecan palygorskites may be the result of diagenesis from dolomite or montmorillonite.

The crystallochemistry of palygorskite

AEM analyses were used to calculate the structural formulae for some Yucatecan palygorskites (Y1a, Y3, Y7, Y8 and Y13). The results are compared with other references and with the ideal palygorskite. In Yucatecan palygorskites, the tetrahedral sheet presents only a very small

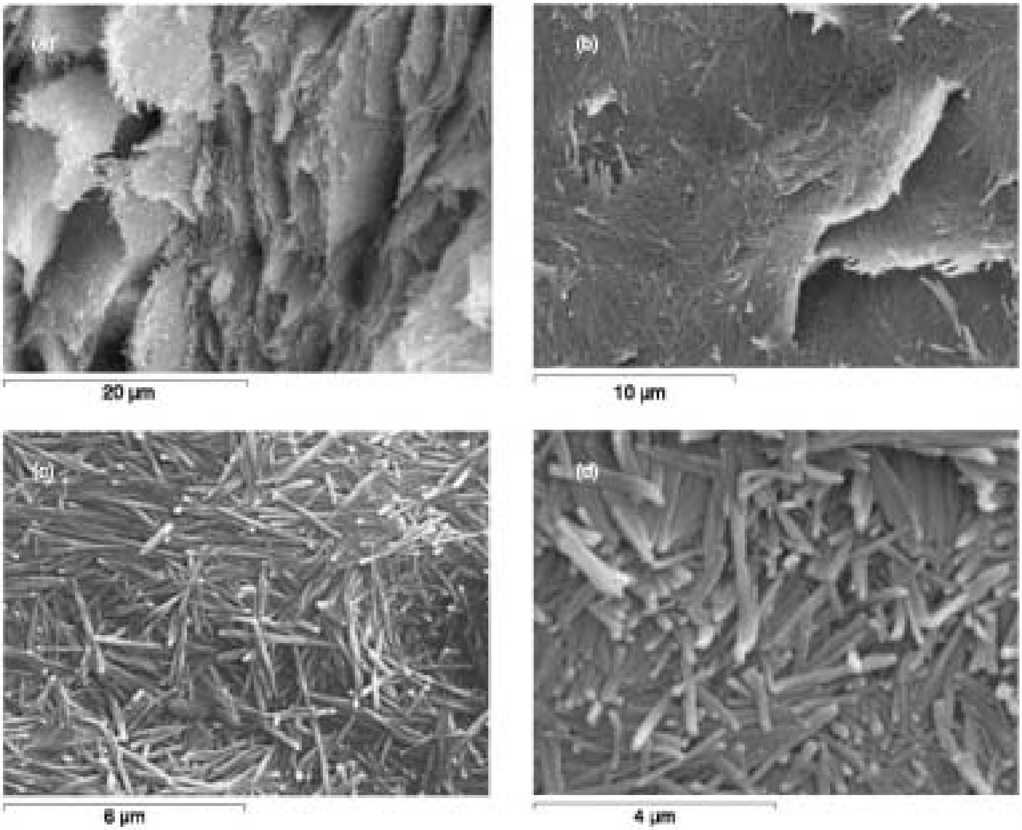

Figure 4 *SEM micrographs. (a) Sample Y8: the arrangement of the fibres forming parallel planes. (b) Sample Y7: a general view of a planar surface that is formed by interbred fibres. (c, d) Samples Y7 and Y 13, respectively. The characteristic fibrous morphology of palygorskite is evident, showing also a high purity. The palygorskite is structured as superposed flat layers of fibres. The fibres are randomly oriented in the layer planes.*

amount of Si substituted by Al ($7.86 < [Si] < 8.04$, where the brackets represent the atomic content). The contents in the octahedral cations are $1.44 < [Al_{(VI)}] < 1.67$, $2.18 < [Mg] < 2.34$ and $0.14 < [Fe^{3+}] < 0.28$. The similarity among these Yucatecan samples when compared with the reference samples from other locations is demonstrated in Figure 5. The compositional results (see Table 2) clearly show that the palygorskites coming from the different localities in Yucatán have similar octahedral contents, and that they are also similar to other palygorskites, such as those from Attapulgus or Torrejón (Suárez *et al.* 2007). This confirms the previous results inferred from XRD. All these palygorskites belong to Type II (Suárez *et al.* 2007), characterized by an $Al_{(VI)}$ content between 1 and 2, and with the number of octahedral cations close to 4 (i.e., one vacant octahedral position).

These results give an average formula for the Yucatecan palygorskite as $(Si_{7.96}Al_{0.07})O_{20}(Al_{1.59}Fe^{3+}_{0.20}Mg_{2.25})(OH)_2(OH_2)_4Ca_{0.02}Na_{0.02}K_{0.04}\cdot 4(H_2O)$, to be compared with: (i) the ideal palygorskite $Si_8O_{20}(Al_2Mg_2)(OH)_2(OH_2)_4\cdot 4(H_2O)$; (ii) the formula in de Pablo-Galán (1996) $(Si_{7.61}Al_{0.39})O_{20}(Al_{1.54}Fe^{3+}_{0.19}Fe^{2+}_{0.04}Mg_{2.19})(OH)_2(OH_2)_4Ca_{0.15}Na_{0.17}K_{0.11}\cdot 4(H_2O)$; and (iii) the

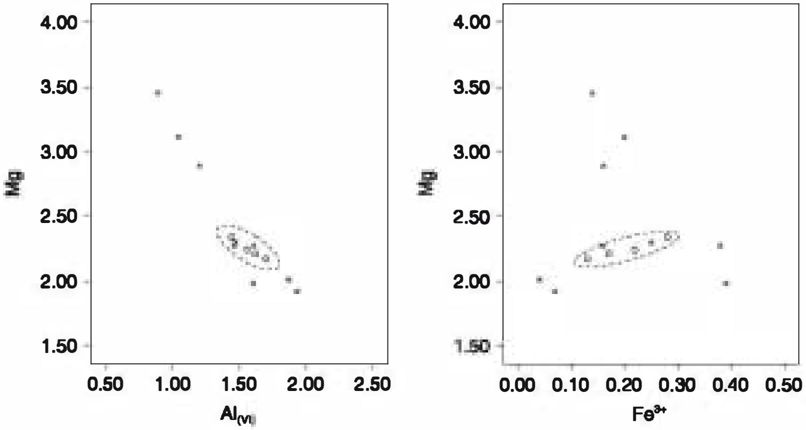

Figure 5 *Bivariate plots representing the number of octahedral cations (per half-unit cell) obtained from AEM of of Yucatán samples (●) and other reference palygorskites (×).*

Table 2 *The composition of six samples of Yucatecan palygorskites obtained by AEM: τ, Tetrahedral sites; o, octahedral sites; STDV, standard deviation; N, number of measurements; $Al_{(IV)}$, aluminium in a tetrahedral site; $Al_{(VI)}$, aluminium in an octahedral site*

	Si	*$Al_{(IV)}$*	*Στ*	*$Al_{(VI)}$*	*Fe^{3+}*	*Mg*	*Ti*	*Σo*	*Ca*	*K*	*Na*
Y0	7.86	0.14	8.00	1.56	0.22	2.24	0.01	4.03	0.03	0.10	
STDV, *N* = 15	0.13	0.12	0.02	0.20	0.05	0.22	0.01	0.13	0.02	0.10	0.01
Y1a	7.95	0.07	8.02	1.67	0.16	2.23		4.06	0.03		
STDV, *N* = 15	0.10	0.06	0.05	0.13	0.06	0.20		0.11	0.06		
Y3	8.04	0.02	8.07	1.55	0.14	2.32	0.01	4.01	0.01	0.04	0.03
STDV, *N* = 15	0.14	0.04	0.12	0.11	0.04	0.18		0.11	0.02	0.04	0.06
Y7	7.97	0.06	8.03	1.62	0.17	2.21		4.01	0.03	0.01	0.07
STDV, *N* = 15	0.12	0.09	0.05	0.13	0.08	0.15		0.14	0.04	0.01	0.10
Y8	7.92	0.09	8.01	1.67	0.20	2.18	0.01	4.05	0.01	0.07	
STDV, *N* = 12	0.10	0.09	0.02	0.08	0.03	0.13		0.08	0.00	0.03	
Y13	7.99	0.04	8.03	1.44	0.28	2.34		4.07	0.01		0.02
STDV, *N* = 9	0.12	0.14	0.05	0.14	0.11	0.17		0.13			
Mean Yucatán	7.96	0.07	8.03	1.59	0.20	2.25	<0.01	4.04	0.02	0.04	0.02

formula calculated using the major element concentrations resulting from geochemistry analysis (see the next paragraph) $(Si_{7.78}Al_{0.22})O_{20}(Al_{1.58}Fe^{3+}_{0.22}Mg_{2.35})(OH)_2(OH_2)_4Ca_{0.11}Na_{0.09}K_{0.02}\cdot 4(H_2O)$. The differences found do not seem to be dramatic considering the diversity of techniques employed and the intrinsic compositional variability of the palygorskite. Moreover, it is remarkable that the octahedral content is similar for the three formulae.

Lastly, it should be noted that the AEM method needs only a microsample, which makes it very suitable technique for analysis of Maya blue pigments from archaeological samples. The data presented in Table 2 will allow us to know whether or not the archaeological pigments present a crystal chemistry that is compatible with the Yucatán one.

Table 3 *Concentrations resulting from geochemical analysis of the Yucatecan palygorskites (Y0, Y1a, Y7, Y8 and Y13) and other palygorskites from different origins. Numbers shown in italics are upper limit*

	Z	*Y0*	*Y1a*	*Y7*	*Y8*	*Y13*	*LISL*	*TOR*	*E11*	*ATT*	*SNE*	*BERC*	*TRA*
Major (%)													
Si	14	24.662	25.470	24.770	25.862	25.578	25.559	27.007	12.539	25.484	25.386	23.733	26.124
Al	13	5.396	6.718	4.142	5.406	4.877	6.237	3.883	1.714	6.099	6.136	8.152	3.793
Fe	26	1.105	1.434	1.294	1.574	1.546	0.615	1.700	0.650	2.721	0.783	4.022	1.238
Mn	25	0.003	0.002	0.006	0.006	0.003	0.018	0.067	0.032	0.094	0.037	0.072	0.263
Mg	12	6.772	6.006	7.266	6.259	6.729	5.481	4.908	3.202	5.294	5.355	2.810	8.104
Ca	20	0.343	0.264	1.272	0.114	0.765	0.207	3.130	22.270	0.993	0.465	2.273	0.121
Na	11	0.059	0.045	0.015	0.185	0.185	0.045	0.126	0.022	0.134	0.141	0.245	0.045
K	19	0.656	0.208	0.473	0.531	0.091	0.274	0.664	0.465	1.038	0.249	1.868	0.149
Ti	22	0.152	0.192	0.103	0.143	0.127	0.207	0.278	0.071	0.269	0.014	0.349	0.045
P	15	0.004	0.004	0.004	0.013	0.004	0.031	0.009	0.013	0.009	0.009	0.022	0.048
Trace (μg g^{-1})													
Be	4	*<1*	*<1*	1	1	*<1*	*<1*	2	*<1*	2	1	3	1
Sc	21	5	7	6	7	6	16	6	2	9	6	13	4
V	23	74	90	38	27	63	167	41	39	75	75	124	14
Cr	24	40	100	30	50	40	30	40	*<20*	50	*<20*	80	*<20*
Co	27	1	1	5	3	2	4	8	*<1*	10	34	24	34
Ni	28	20	*<20*	40	40	20	*<20*	*<20*	*<20*	20	*<20*	40	100
Cu	29	*<10*	*<10*	20	*<10*	*<10*	10	10	*<10*	10	*<10*	30	40
Zn	30	*<30*	*<30*	*<30*	40	*30*	*30*	40	*<30*	*<30*	*<30*	60	30
Ga	31	12	17	13	14	12	32	11	5	14	23	22	22
Ge	32	0.7	1	1.1	1.3	0.6	0.8	1	1.2	1	2.5	1.9	10
As	33	*<5*	8	*<5*	7	*<5*	*<5*	5	*<5*	11	*<5*	9	*5*
Rb	37	36	13	36	41	11	11	49	28	66	9	130	11
Sr	38	8	6	18	7	18	30	77	90	42	18	91	8
Y	39	1.2	1.9	1.5	5.6	1.1	1.7	21.4	6.6	20.8	0.8	30.2	34.4
Zr	40	153	224	153	135	104	45	165	38	129	11	152	65
Nb	41	7.2	9.1	6.2	7.6	4.2	6.9	7.9	3	7.2	0.6	11.9	13.2
Mo	42	*<2*	*<2*	*<2*	*<2*	*<2*	*<2*	*<2*	*<2*	*<2*	*<2*	*<2*	*<2*
Ag	47	*<0.5*	*<0.5*	*<0.5*	*<0.5*	*<0.5*	*<0.5*	*<0.5*	*<0.5*	*<0.5*	*<0.5*	*<0.5*	*<0.5*
In	49	*<0.1*	*<0.1*	*<0.1*	*<0.1*	*<0.1*	*<0.1*	*<0.1*	*<0.1*	*<0.1*	*<0.1*	*<0.1*	*<0.1*
Sn	50	2	4	2	3	3	*<1*	3	2	3	*<1*	5	2
Sb	51	*<0.2*	*<0.2*	2.2	*<0.2*	*<0.2*	*<0.2*	*<0.2*	*<0.2*	*<0.2*	3.3	*<0.2*	*<0.2*
Cs	55	2.9	1.3	2.2	2.9	1.3	0.2	4.2	1.8	6.1	0.3	9.9	1.8
Ba	56	18	21	33	44	26	53	495	121	546	15	564	33
Hf	72	3.9	5.7	3.7	4.1	2.8	0.9	4.4	1.2	3.3	0.2	4.1	1.4
Ta	73	0.93	0.94	0.47	0.75	0.43	0.48	0.88	0.39	0.8	0.03	1.11	0.43
W	74	0.7	0.6	0.7	*<0.5*	0.7	3.2	1.3	1.8	2.9	*<0.5*	2	2
Tl	81	0.12	*<0.05*	0.1	0.16	0.08	*<0.05*	0.32	0.22	0.53	0.15	0.86	0.39
Pb	82	*<5*	*<5*	*<5*	*<5*	*<5*	*<5*	8	*<5*	11	*<5*	23	*<5*
Bi	83	0.2	0.9	0.2	0.4	0.4	0.1	0.5	*<0.1*	0.6	*<0.1*	1	0.2
Th	90	3.3	8.05	3.92	11.3	2.61	0.53	8.7	5.01	8.21	0.39	13.6	6.05
U	92	0.92	0.54	0.26	0.46	0.21	0.2	2	0.74	1.69	0.22	1.76	0.21
LREE (μg g^{-1})													
La	57	1.83	1.93	1.81	10	1.45	4.36	25	10.7	25.9	0.57	35.3	15.9
Ce	58	3.64	4.41	6.02	17.3	2.97	12.8	51.6	30.3	52.5	2.47	84.8	29.4
Pr	59	0.39	0.44	0.48	3.05	0.32	1.22	6.38	2.62	6.24	0.15	8.28	3.64
Nd	60	1.24	1.56	1.59	10.3	1.08	4.56	23.6	9.25	23	0.51	30	13.7
Sm	62	0.22	0.29	0.29	1.93	0.2	0.79	4.52	1.9	4.5	0.11	5.82	3.02

Table 3 *Continued*

	Z	*Y0*	*Y1a*	*Y7*	*Y8*	*Y13*	*LISL*	*TOR*	*E11*	*ATT*	*SNE*	*BERC*	*TRA*
HREE ($\mu g\ g^{-1}$)													
Eu	63	0.039	0.053	0.052	0.223	0.036	0.248	0.899	0.254	0.97	0.024	1.41	0.413
Gd	64	0.15	0.23	0.22	1.3	0.14	0.51	3.53	1.53	3.81	0.11	5.2	3.13
Tb	65	0.03	0.05	0.04	0.21	0.03	0.07	0.6	0.25	0.69	0.02	0.97	0.63
Dy	66	0.2	0.31	0.23	1.14	0.19	0.38	3.51	1.39	3.73	0.1	5.81	4.32
Ho	67	0.04	0.07	0.05	0.22	0.04	0.06	0.68	0.25	0.72	0.02	1.14	0.98
Er	68	0.15	0.24	0.16	0.67	0.15	0.16	1.97	0.69	2.15	0.06	3.3	3.26
Tm	69	0.032	0.045	0.032	0.119	0.026	0.02	0.291	0.102	0.321	0.01	0.484	0.527
Yb	70	0.25	0.33	0.25	0.89	0.21	0.11	1.88	0.62	2.08	0.08	2.99	3.6
Lu	71	0.039	0.059	0.053	0.162	0.04	0.015	0.277	0.087	0.302	0.014	0.422	0.58

The geochemistry of palygorskite

The statistical analysis of the chemical data (concentration of major elements) as well as the trace elements may classify the samples in groups with different chemical fingerprints related to the geology of the deposits. Five Yucatecan samples, Y0, Y1a, Y7, Y8 and Y13, were selected for this study, together with seven palygorskites from other origins. The aim is to test whether all samples from Yucatán have similar contents in trace elements or, on the contrary, whether their contents in trace elements vary from one sample to another, thus depending on the deposit.

The Yucatán samples are characterized by a low content in rare earth elements, both for light rare earth elements (LREE) and for heavy ones (HREE) (Table 3). Also, Y and U contents are particularly low in Yucatecan samples. In contrast, Hf and Zr are more concentrated in Yucatecan palygorskites than in the other palygorskites studied. Amold *et al.* (2007) found discrepancies in values of concentrations in Hf and Zr measured using two different techniques, one more sensitive to the bulk (INAA), and the other to the surface (LA–ICP–MS). They suggested the possible presence of minute zircon grains, more represented in the bulk. The sample from the *cenote* in Sacalum presents the highest values (17 µg g^{-1} for Ce, 10 µg g^{-1} for La and Nd), several orders of magnitude greater than the others. Also, the content in Y is especially low in these samples. The values of both the trace elements and major elements are good parameters to distinguish between Yucatecan and non-Yucatecan samples, as seen in Figure 6. Moreover, it is also possible to differentiate the Yucatán group when looking at several bivariate plots (Fig. 7) or in a scatterplot matrix (Fig. 8). Therefore, the concentration of both trace and major elements in palygorskite defines a chemical fingerprint that characterizes the samples coming from Yucatán.

Arnold *et al.* (2007) proposed to use trace element analysis (INAA and LA–ICP–MS) for provenance analysis of Maya blue pigment. They analysed many samples, most of them from the Yucatán area, and distinguished provenance groups within the Yucatán peninsula (Sacalum, Chapab and Uxmal) when looking at the bivariate plots of Rb versus V, Ni or Mn. Although we have analysed only one representative of each origin (see Table 3), we have verified that they present a similar trend. Our Y0, Y7 and Y8 samples ($1.4 < \log 10([\mathrm{Rb}]) < 1.8$) group quite well with Amold's Sacalum group, and our Y1a and Y13 are close to his Uxmal group. This is consistent with the geographic origin. The Yucatecan samples, as compared with all the rest,

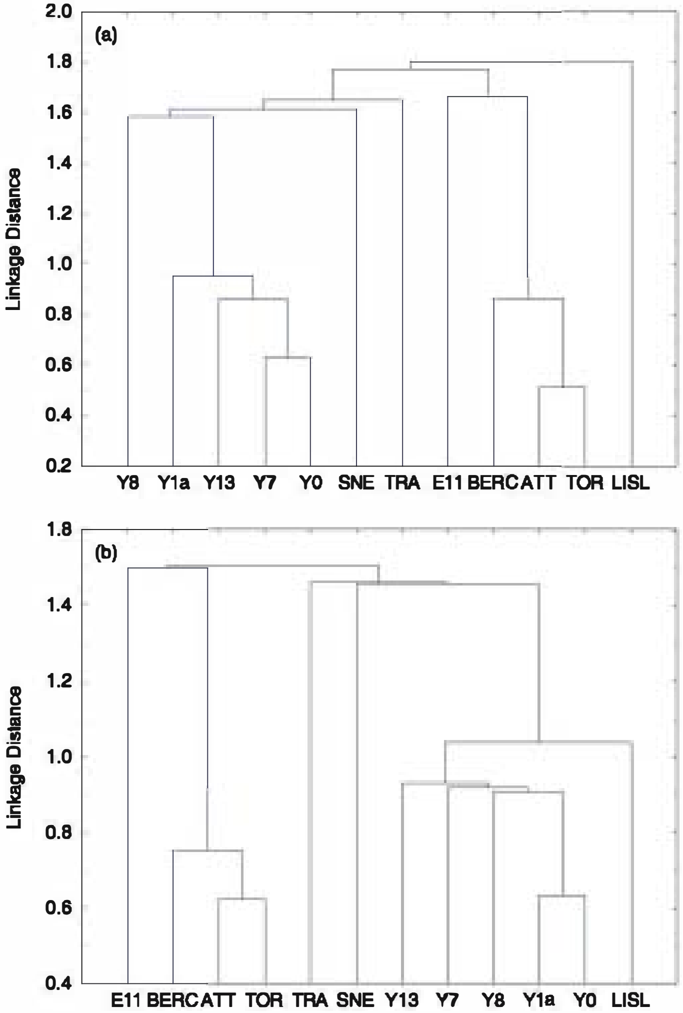

Figure 6 *Dendrograms built using the geochemistry analysis (log$_{10}$ of concentrations) of different palygorskites from Yucatan (Y0, Y1a, Y7, Y8 and Y13) and other origins. (a) A dendrogram built using all trace elements except U, W, Yb, Er, Dy, Gd and Sm. (b) A dendrogram built using major elements. It can be appreciated that Yucatecan palygorskites are always grouped together.*

are particularly low in Mn, and this could be a simple fingerprint for addressing or excluding Yucatecan origins. In addition to Mn, the Yucatecan samples are different from the Attapulgus one (the only one from the same continent) because they are poor in several other elements (Ti, Sr, Y, Ba, W and Pb).

SUMMARY AND CONCLUSIONS

Several palygorskites of great purity have been collected in several places in the Yucatán peninsula, all located in a radius of 40 km around the archaeological site of Uxmal. Some of

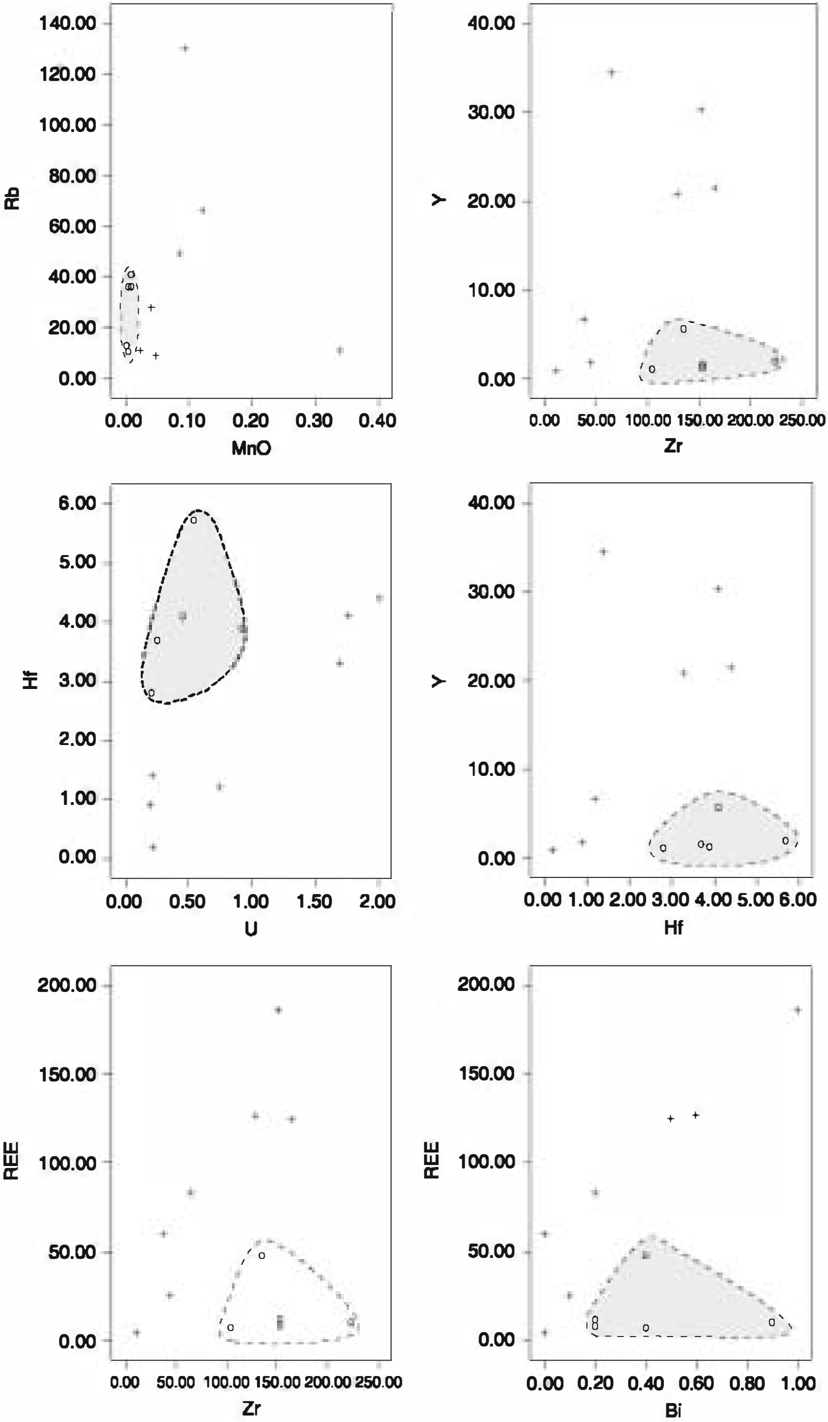

Figure 7 *Bivariate plots representing the trace element concentrations corresponding to data from chemical analyses of Yucatecan samples (●) and other palygorskites used for comparison (+).*

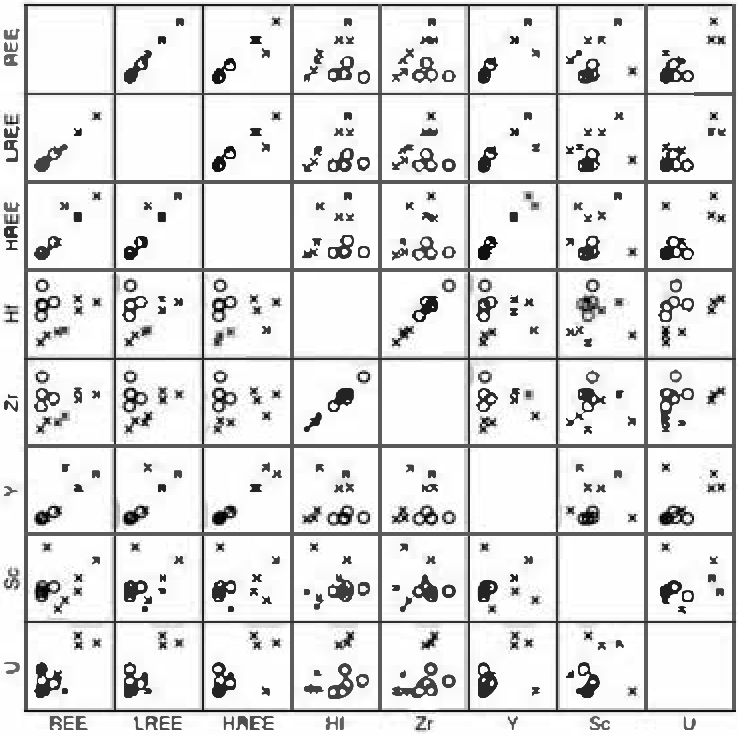

Figure 8 A scatterplot matrix representing the concentrations of trace elements, comparing Yucatecan samples (●) with palygorskites from other locations (x). REE, rare earth elements; LREE, light rare earth elements; HREE, heavy rare earth elements.

these places were well documented, but others are reported here for the first time. The abundance of palygorskite in the samples collected allows us to affirm that palygorskite is a frequent mineral in the studied area and can be easily found at almost surface level. From this fact, it can be argued that the ancient Maya could have extracted palygorskite from different places in this area. As palygorskite occurs close to the surface, evidence of the extraction could have been removed by the effects of erosion and vegetation over a number of centuries. This supports the idea that palygorskite is widespread in Yucatán, at least in the studied area, as discussed by Littmann (1982) and Arnold *et al.* (2007).

All of the Yucatecan palygorskites present very similar diffractograms, and show marked differences with respect to other palygorskites analysed. This implies compositional and structural homogeneity, making it impossible from this point of view to separate them into provenance groups within Yucatán, but they can be easily differentiated from other origins. The crystallochemical analysis confirmed this result and allowed us to obtain a mean compositional formula: $(Si_{7.93}Al_{0.07})O_{20}(Al_{1.59}Fe^{3+}_{0.20}Mg_{2.25})(OH)_2(OH_2)_4Ca_{0.02}Na_{0.02}K_{0.04}\cdot 4(H_2O)$. Yucatecan palygorskites also contain trace elements that differentiate them easily from the other origins. Eventually, careful analysis of trace elements could be used to further determine the origin within several groups in the Yucatán peninsula, as suggested by Arnold *et al.* (2007). The results presented here will be used when studying archaeological Maya blue pigments in order to check whether the palygorskite used in the pigment, either from Maya or other Mesoamerican regions, could have originated from this area.

ACKNOWLEDGEMENTS

The samples were collected in a visit to Yucatán during the sabbatical leave of MSR at the Universidad Autónoma Metropolitana-Iztapalapa (Mexico), which is acknowledged for financial support. Xim Bokhimi provided us with the sample from Tepakan, Campeche. We also acknowledge financial support from the Spanish CICYT (project CGL2006-09843) and the Servicio de Investigación de la UCM (Grupo 9103B6).

REFERENCES

Arnold, D. E., 1998, Ceramic ethnoarchaeology at Ticul, Yucatan, Mexico, *The Society for Archaeological Sciences Bulletin*, **21**; http://www.socarchsci.org/bulletin/9902/9902j.htm

Arnold, D. E., 2005, Maya blue and palygorskite: a second possible Pre-Columbian source, *Ancient Mesoamerica*, **16**, 51–62.

Arnold, D. E., and Bohor, B. F., 1975, Attapulgite and Maya blue. An ancient mine comes to light, *Archaeology*, **28**, 23–9.

Arnold, D. E., Neff, H., Glascock, M. D., and Speakman, R. J., 2007, Sourcing the palygorskite used in Maya blue: a pilot study comparing the results of INAA and LA–ICP–MS, *Latin American Antiquity*, **18**(1), 44–58.

Bohor, B. F., 1975, *Attapulgite in Yucatan*, Instituto de Geología, UNAM, Mexico DF.

Chiari, G., Giustetto, R., and Ricchiardi, G., 2003, Crystal structure refinement of palygorskite and Maya blue from molecular modelling and powder synchrotron diffraction, *European Journal of Mineralogy*, **15**(1), 21–33.

Chirst, C. L., Hathaway, J. C., Hostler, P. B., and Shepard, A. O., 1969, Palygorskite: new X-ray data, *American Mineralogist*, **54**, 198–205.

Chisholm, J. E., 1990, An X-ray powder-diffraction study of palygorskite, *Canadian Mineralogist*, **28**, 329–39.

Chisholm, J. E., 1992, Powder-diffraction patterns and structural models for palygorskite, *Canadian Mineralogist*, **30**, 61–73.

de Pablo-Galán, L., 1996, Palygorskite in Eocene–Oligocene lagoonal environment, Yucatán, Mexico, *Revista Mexicana de Ciencias Geológicas*, **13**(1), 94–103; http://satori.geociencias.unam.mx/13-1/(6)de_Pablo.pdf

Folan, W. J., 1969, Sacalum, Yucatan: a pre-hispanic and contemporary source of attapulgite, *American Antiquity*, **34**(2), 182–3.

García Romero, E., Suárez, M., Oyarzun, R., López-García, J. A., and Regueiro, M., 2006, Formation of palygorskite in secondary faults from a large shear zone of Miocene age (Serrata de Níjar, SE Spain), *Clays and Clay Minerals*, **54**(3), 324–32.

Gettens, R. J., 1962, An unsolved problem in ancient pigments, *American Antiquity*, **7**(4), 557–64.

Giustetto, R., and Chiari, G., 2004, Crystal structure refinement of palygorskite from neutron powder diffraction, *European Journal of Mineralogy*, **16**, 521–32.

Giustetto, R., Llabres i Xamena, F. X., Ricchiardi, G., Bordiga, S., Damin, A., Gobetto, R., and Chierotti, M. R., 2005, Maya blue: a computational and spectroscopic study, *Journal of Physical Chemistry B*, **109**(41), 19360–8.

Isphording, W. C., 1984, The clays from Yucatán, Mexico; a contrast in genesis, in *Palygorskite–sepiolite occurrences, genesis and uses* (eds. A. Singer and E. Galán), 75–86, Developments in Sedimentology 37, Elsevier, Amsterdam.

Isphording, W. C., and Wilson, E. M., 1974, The relationship of 'volcanic ash,' sak lu'um, and palygorskite in northern Yucatan Maya ceramics, *American Antiquity*, **39**(3), 483–8.

Littmann, E. R., 1982, Maya blue—further perspectives and the possible use of indigo as the colorant, *American Antiquity*, **47**(2), 404–8.

Morán-Zenteno, D., 1994, *The geology of the Mexican Republic*, AAPG Studies in Geology, American Association of Petroleum Geologists, Tulsa, OK.

Reyes-Valerio, C., 1993, *De Bonampak al Templo Mayor. El azul maya en Mesoamerica*, siglo XXI editores, Mexico DF.

Sabloff, J. A., and Rathje, W. L., 1975, The rise of a Maya merchant class, *Scientific American*, **233**(4), 72–83.

Sánchez del Río, M., Martinetto, P., Reyes-Valerio, C., Dooryhée, E., and Suárez, M., 2006a, Synthesis and acid-resistance of the Maya blue pigment, *Archaeometry*, **48**, 115–30.

Sánchez del Río, M., Picquart, M., Haro-Poniatowski, E., van Elslande, E., and Uc, V. H., 2006b, On the Raman spectrum of Maya blue, *Journal of Raman Spectroscopy*, **37**, 1046–53.

Sánchez del Río, M., Sodo, A., Eeckhout, S., Neisius, T., Martinetto, P., Dooryhée, E., and Reyes-Valerio, C., 2005, Fe K-edge XANES of Maya blue pigment, *Nuclear Instruments and Methods B*, **238**, 50-4.

Scarborough, V. L., and Gallopin, G. G., 1994, A water storage adaptation in the Maya lowlands, *Science*, **251**(4), 658–62.

Shepard, A. O., 1962, Maya blue: alternative hypothesis, *American Antiquity*, **27**, 565–6.

Shepard, A. O., and Gottlieb, H. B., 1962, *Maya blue: alternative hypothesis*, Notes from a Ceramic Laboratory **1**, Carnegie Institution of Washington, Washington, DC.

Suárez, M., and García Romero, E., 2006, Macroscopic palygorskite from volcanic complex of Lisbon, *European Journal of Mineralogy*, **18**(1), 119–26.

Suárez, M., García-Romero, E., Sánchez del Río, M., Dooryhée, E., and Martinetto, P., 2007, The effect of the octahedral cations on the dimensions of the palygorskite cell, *Clay Minerals*, **42**, 287–97.

Tagle, A. A., Paschinger, H., Richard, H., and Infante, G., 1990, Maya blue: its presence in Cuban Colonial wall paintings, *Studies in Conservation*, **35**, 156–9.

Viseras, C., and López-Galindo, A., 1999, Pharmaceutical applications of fibrous clays (sepiolite and palygorskite), *Applied Clay Science*, **14**, 69–82.

Wolfgang, S., Gerta, K., Thierry, A., Markus, H., Doris, S., Georg, I., and Utz, K., 2004, Yaxcopoil-1 and the Chicxulub impact, *International Journal of Earth Sciences*, **V93**(6), 1042–65.